# Structure in the cross section for the reaction $^{208}$Pb($\gamma$,$n$)

S. N. Belyaev,[1)] O. V. Vasil'ev,[1)] V. V. Voronov, A. A. Nechkin,[1)]
V. Yu. Ponomarev, and V. A. Semenov[1)]

*Joint Institute for Nuclear Research, Dubna*
(Submitted 13 September 1991)
Yad. Fiz. **55**, 289–297 (February 1992)

The cross section for the reaction $^{208}$Pb($\gamma$,$n$) has been studied by a bremsstrahlung method in a search for intermediate structure in the interval from the reaction threshold up to 25 MeV. Structure of this sort has been found in the low-energy region. The experimental data are compared with results calculated from the quasiparticle–phonon model.

## 1. INTRODUCTION

The very active research on the giant multipole resonances in various reactions has resulted in the accumulation of extensive experimental data on the integral characteristics of these reactions.[1–3] The photoabsorption reaction has been the basis for one of the most effective methods for studying giant dipole resonances. There is the hope that improvements in the resolution of the corresponding experiments would be rewarded with new information on the fine structure of giant dipole resonances.[4,5] In particular, substructure has been discovered in several nuclei through studies of the low-energy region of the giant dipole resonance.[4–6]

The presence of substructure in the photoabsorption cross sections in the vicinity of magic nuclei was mentioned in Ref. 7. Theoretical work on the giant resonances has established that they are damped primarily as the result of a coupling between simple and complex configurations.[7–13] This coupling is relatively weak in the vicinity of magic nuclei. As a result, a substructure arises in the low-energy region, where the density of levels is considerably lower than near the peak of the giant dipole resonance.[7]

Our objectives in the present study were to learn about the substructure of $^{208}$Pb through photoneutron experiments and to compare the resulting data with the results of microscopic calculations based on the quasiparticle–phonon model.[14–16]

## 2. EXPERIMENTAL APPARATUS AND PROCEDURE

The reliability of results found by the bremsstrahlung method depends on: 1) keeping the operation of the accelerator and the measurement apparatus stable within the necessary range for a long time; 2) selecting a correct method for solving the inverse problem in reconstructing the cross section from the measured photoneutron yields.

The use of a multichannel method[17] and the maintenance of a given maximum bremsstrahlung energy $E_{\gamma\,\max}$ within $\approx$5 keV (Ref. 18) made it possible to carry out the measurements with a step suitable for the given resolution level over the long time required to build up a statistical base. Model-based calculations with parameter values close to the real values, with discretization of the continuous function at steps $\approx$50 keV, made it possible to detect structural features with a width of 150–200 keV. The uncertainty in the energy due to the duration of the displacement of the electron beam onto the accelerator target has a smoothing effect. This uncertainty reaches 25–30 keV at an energy of 25 MeV. A calibration of the energy scale on the basis of the thresholds for photoneutron reactions and the slope change at 17.25 MeV in the photoneutron yield from oxygen results in an error $\approx$20 keV.

Neutrons moderated in paraffin were detected by $BF_3$ counters with an overall efficiency of 20% (Ref. 19). The effect of fluctuations in the intensity of the $\gamma$ beam was suppressed by normalizing the detected neutrons to the dose, which was measured by a scintillation dosimeter for each $\gamma$ pulse.[20] The data were sent to a graphics display for visual monitoring during the experiment.

Data on the $^{208}$Pb($\gamma$,$n$) reaction are given in Ref. 5 at steps of 25 keV at energies up to 9 MeV and at steps of 50 keV up to 12 MeV. In the present experiment, the energy range was extended to 22 MeV. As a result, the number of channels was increased, and a variable step in $E_{\gamma\,\max}$ was used. For the intervals from the neutron emission threshold $B_n$ up to 8.5 MeV, up to 12 MeV, and above 12 MeV, the steps were 40, 60, and 120 keV, respectively. The energy was scanned by a procedure designed to compensate for the small neutron yield at energies near the threshold by carrying out a large number of measurements in the corresponding channels. The same target, 2.52 g/cm thick, with 99% enrichment, was used in all the measurements.

The results of these measurements consisted of the mean photoneutron yield and the standard deviation at the given points along $E_{\gamma\,\max}$. After corrections for the background and for counting losses, and after a conversion of the yields to dose units, these results were used to find the cross section for the ($\gamma$,$n$) reaction.

## 3. CALCULATION OF THE CROSS SECTIONS FROM THE DATA ON THE PHOTONEUTRON YIELD

When the bremsstrahlung method is used, the ($\gamma$,$n$) cross section is found by solving an inverse problem, specifically, a system of integral equations of the type

$$\int_{B_n}^{E^i_{\gamma\,max}} \Phi(E^i_{\gamma\,max},\ E_\gamma{}^i)\,\sigma_{exp}(E_\gamma)\,dE_\gamma = Y(E^i_{\gamma\,max}). \qquad (1)$$

where $\Phi(E^i_{\gamma\,\max})$ is the shape of the bremsstrahlung spectrum, $Y(E^i_{\gamma\,\max})$ is the reduced photoneutron yield, and $\sigma(E_\gamma)$ is the experimental cross section, which is essentially equal to the sum $\sigma(\gamma,n)+\sigma(\gamma,2n)$, since the other partial cross sections are small.

Since there is a certain error in the raw data for Eq. (1) (these results are estimates based on a limited sample), only an approximate solution can be found. This solution varies

 0038-5506/92/020157-05$05.00 © 1992 American Institute of Physics 

substantially when small changes occur in the raw data. The problem thus falls into the category of ill-posed problems. We used a statistical regularization method[21] to find the cross sections. In this method, the probabilistic nature of the experimental data was taken into consideration. In our case, the values of the measured yield $Y(E^i_{\gamma\max})$ are sample means of random variables. Consequently, they too are random variables. Their deviations from the true values can be specified by means of a distribution of these deviations. We assume that this distribution is Gaussian and that its variance is the same as the experimental variance [in the problem at hand, the same as the variance of the photoneutron yield, $(\Delta Y)^2$]. A solution of Eq. (1) is sought in the ensemble of smooth functions which belong to a certain distribution. The density of this distribution is found as the *a posteriori* probability density of the given solution, $\sigma$, for a given value of $Y$:

$$P(\sigma/Y)=P(\sigma)P(Y/\sigma). \qquad (2)$$

Here $P(\sigma)$ is the *a priori* probability density found by requiring that the information content and smoothness of the solution be minimized, and $P(Y/\sigma)$ is the conditional probability density for the appearance of a given value of $Y$ under the condition for the existence of $\sigma$.

A solution $P(Y/\sigma)$ is found by the method of a maximum *a posteriori* probability density. The error $\Delta\sigma$ is found as the square root of the variance of this distribution.

This method makes is possible to analyze data measured with an arbitrary step in the maximum energy $E_{\gamma\max}$. It takes the weight of each yield point into consideration. It inserts nothing into the reconstructed function which is not present in the experimental data. Note that the raw data contain more comprehensive information on the cross section than is contained in the reconstructed function. The reason for this difference is that there is an average over the structure in the cross section (if such structure exists; whether it does would generally not be known at the outset) because of the finite number of points used in the discretization of the energy scale, if the measurement step is comparable to the widths of this structure.

In the bremsstrahlung method, the ability to resolve structure with a width of 200–600 keV at a step in $E_{\gamma\max}$ on the order of 50 keV is roughly the same as in a method based on a quasimonochromatic beam of $\gamma$ rays with a half-width of 140–200 keV. There are differences, in the smoothness of the cross section and in the extent to which the structure is resolved. These points are very important in the subsequent analysis.

To normalize the cross section to absolute values, we used the ratio of (a) the area under the peak in the $^{142}$Nd cross section according to a calculation based on the parameters of a Lorentzian line, from Ref. 22, to (b) that which we found from data on $^{142}$Nd, obtained under the same experimental conditions as for $^{208}$Pb. The $\sigma(\gamma,2n)$ correction was found by the statistical theory of Ref. 23. Here we made use of a parameter serving as a measure of the density of levels found from a fit to the $\sigma(\gamma,n)$ and $\sigma(\gamma,2n)$ partial cross sections from Ref. 24.

## 4. ANALYSIS OF THE CROSS SECTIONS AND DETERMINATION OF THE PARAMETER VALUES

In order to interpret the experimental cross sections, we need some quantitative information on these cross sections which can be compared with that found in model-based calculations or from other measurements. Various approaches can be taken here, depending on the purpose of the study.

1) One might find parameter values which characterize the cross section as one large peak (or two such peaks, in the case of nuclei having a static deformation), through an approximation of the raw data by a Lorentzian line. The intermediate structure is ignored in this approach. This systematic classification of the parameters has been carried out since Ref. 3, for the $(\gamma,n)$ cross sections found in a beam of quasimonochromatic $\gamma$ rays. The parameter values can then be used as in Ref. 25 (for example), where the systematics was used to derive empirical expressions for the width of giant dipole resonances in spherical and deformed nuclei.

2) The cross section can be represented as a set of resonance lines. The type of line is chosen on the basis of either physical considerations or the actual features of the curve under study. In this case the giant dipole resonance is not treated as a single collective state with a large width (4–6 MeV) but as the envelope of a large number of narrower resonances, which are localized within certain energy intervals. Armed with the characteristics of the structures which shape the cross section, one can determine the actual localization region and estimate the contribution to the integral cross section.

The second of these approaches is preferable for the $^{208}$Pb cross section, with some pronounced structural features on the rising part of the giant dipole resonance. Specification of simply the energy positions of the structural features observed in Refs. 6 and 24–27 is less informative for a comparison with theoretical predictions.

Figure 1 shows the experimental $(\gamma,n)$ cross sections which we will be discussing here. These cross sections differ slightly in the shape of the structure (and even in the presence or absence of the structure, when we note the poorly resolved peak at $\approx$7.43 MeV). These differences confirm that the resolution level depends on the measurement step and on the measurement error.

Table I shows parameter values found by describing the $(\gamma,n)$ cross section by a set of Gaussian lines:

$$\sigma(\gamma,n)=\sum_i \sigma_0{}^i \exp-[(E-E_0{}^i)^2/2\delta_i{}^2], \qquad (3)$$

where $\sigma^i_0$, $E^i_0$, and $\delta_i$ characterize the amplitude, position, and width of the resonances making up the cross section. The quantity $\delta_i$ is the square root of the variance of the corresponding distribution and is related to the width at half-maximum, $\Gamma_i$, by $\Gamma_i = 2.355\delta_i$.

Working from these parameter values, we determined the relative contributions of the peaks to the integral cross section (as percentages). The integral cross section was calculated as the sum of the areas under the Gaussian lines. The absolute values (in millibarn·mega-electron-volts) of the contributions of the individual peaks were specified by the areas under the corresponding Gaussian curves. This decomposition method is dictated by the shape and number of the structural features observed. Attempts to use Lorentzian or Breit–Wigner lines yielded unsatisfactory results. If one assumes that a main peak, with a crest coinciding with the maximum of the cross section, is formed by one such line, then it is not possible to completely resolve the structure on the leading slope, because of the large width of this peak.

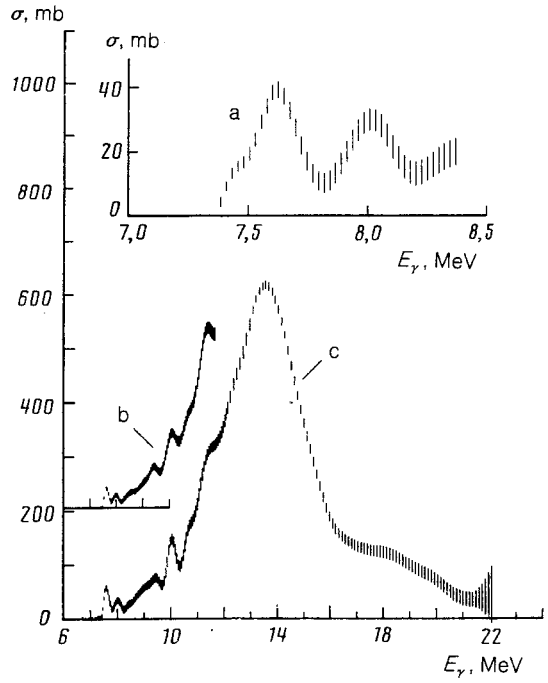


FIG. 1. Cross section for the reaction $^{208}$Pb($\gamma$,$n$): a—measurement step 25 keV; b—measurement step 50 keV; c—measurement steps 40, 60, and 120 keV for the intervals from the photoneutron threshold up to 9 MeV, up to 12 MeV, and above 12 MeV.

## 5. COMPARISON WITH THEORY

Theoretical calculations were carried out on the basis of the quasiparticle–phonon model, which is described in detail in Refs. 14–16. In this model, with an interaction between simple (one-phonon) and complex (two-phonon) configurations, the wave function of the excited state of an even–even nucleus is

$$\Psi_\nu(JM)=\Big\{\sum_i R_i(J\nu)Q^+_{JMi} + \sum_{\lambda i\lambda' i'} P^{\lambda\lambda' i'}_{Mi}(J\nu)\,[Q^+_{\lambda\mu i}Q^+_{\lambda'\mu' i'}]_{JM}\Big\}\Psi_0, \qquad (4)$$

where the operator $Q^+_{\lambda\mu i}$ creates a phonon of multipolarity $\lambda$ with projection $\mu$, ordinal number $i$, and energy $\omega_{\lambda i}$. The latter is found by solving an equation of the random-phase approximation. In addition, $\Psi_0$ is the phonon vacuum, adopted as the ground state of the even–even nucleus.

The energies of the excited states $\eta_{J\nu}$ described by the wave function (4) and also the coefficients $R$ and $P$ were found by solving the corresponding secular equation.[16] For intermediate and high excitation energies, for which the level density is fairly high, it is convenient to use a response function or the equivalent strength function

$$b(\Phi,\nu)=\sum_\nu |\Phi_{J\nu}|^2 \frac{1}{2\pi}\frac{\Delta}{(\eta-\eta_{J\nu})^2+\Delta^2/4} \qquad (5)$$

where $\Phi_{J\nu}$ is the excitation amplitude of the state $\Psi_\nu(JM)$ in the physical process under consideration, and $\Delta$ is an averaging interval. The strength-function method is described in detail in Ref. 16. The photoabsorption cross sections are directly related to the corresponding strength functions. For the average cross section for electric dipole photoabsorption, for example, we can use the expression[7]

$$\sigma_{\gamma t}(E_\gamma)=4{,}025E_\gamma b(E1, E_\gamma), \qquad (6)$$

where $\sigma_{\gamma t}$ is in millibarns, $E_\gamma$ is the energy of the $\gamma$ ray in mega-electron-volts, and $b(E1,E_\gamma)$ is expressed in units of $e^2\cdot$fm$^2$.

In the numerical calculations we used the GIRES program.[28] We used the one-particle Woods–Saxon potential from our previous study.[29] This spectrum is a modification of that found with the parameter values of Ref. 30. It was adjusted in such a way that the energies of the low-lying collective levels, the probabilities for electromagnetic transitions from these states to the $^{208}$Pb ground state, and the energies and spectroscopic factors of the levels of adjacent odd nuclei could all be described with the wave functions of the quasiparticle–phonon model. At the same time, we found the constants of the dipole–dipole and multipole–multipole interaction, in Bohr–Mottelson form. The ratios of the isoscalar constants of the residual forces to the pseudovector constants were determined from the position of the giant dipole resonance. The resulting one-particle spectrum includes all the quasistationary levels up to the centrifugal barrier with the given $l\leqslant 9$. That this basis is sufficiently comprehensive was confirmed by the fact that it correctly describes the probabilities for electromagnetic transitions without the need to introduce effective charges. The results of our calculations of the integral characteristics of the giant resonances in $^{208}$Pb (Refs. 31 and 32) agree well with results found

TABLE I. Parameters of the representation of the photoneutron cross section by a set of Gaussian lines; contributions of the individual resonances to the integral cross section.

| $\sigma_0^i$, mb | $E_0^i$, MeV | $\delta_0^i$, MeV | $\Gamma_i$, MeV | Contribution | |
|---|---|---|---|---|---|
| | | | | mb·MeV | % |
| 61±2 | 7,60±0,01 | 0,095±0,003 | 0,22 | 14,3 | 0,49 |
| 31±3 | 8,00±0,02 | 0,135±0,014 | 0,32 | 10,5 | 0,36 |
| 31±4 | 8,64±0,06 | 0,304±0,026 | 0,72 | 23,7 | 0,81 |
| 50±4 | 9,14±0,05 | 0,235±0,015 | 0,55 | 29,3 | 1,00 |
| 51±6 | 9,47±0,03 | 0,141±0,015 | 0,33 | 17,9 | 0,61 |
| 133±3 | 10,03±0,02 | 0,215±0,018 | 0,51 | 71,7 | 2,45 |
| 76±22 | 10,63±0,03 | 0,176±0,041 | 0,41 | 33,7 | 1,15 |
| 179±4 | 11,33±0,03 | 0,422±0,076 | 0,99 | 189,4 | 6,47 |
| 48±15 | 12,20±0,10 | 0,260±0,076 | 0,61 | 31,0 | 1,06 |
| 618±4 | 13,56±0,02 | 1,227±0,063 | 2,89 | 1902,6 | 65,00 |
| 54±4 | 16,00±0,10 | 0,834±0,040 | 1,96 | 114,0 | 3,86 |
| 117±3 | 18,20±0,08 | 1,688±0,044 | 3,98 | 494,7 | 16,90 |

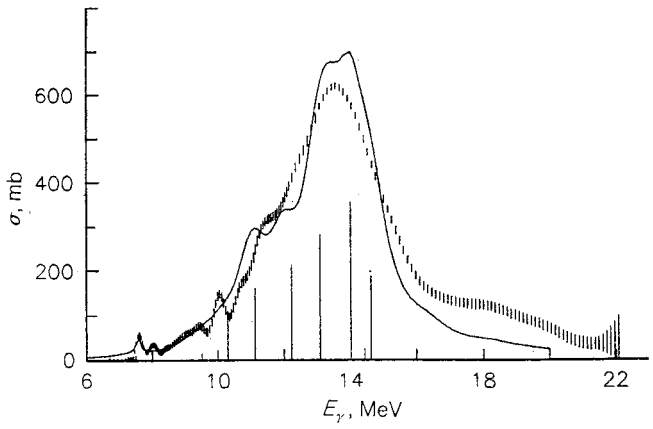


FIG. 2. Photoneutron cross sections of $^{208}$Pb. Points—experimental; solid line—theoretical, with $\Delta = 1$ MeV. The vertical lines are results (in arbitrary units) calculated in the random-phase approximation.

through an exact consideration of the continuum.[9,12]

Let us first take a look at the theoretical description of the integral characteristics of the giant dipole resonance in $^{208}$Pb. For the energy interval 10.0–17.0 MeV, we find $\overline{E}_x = 13.35$ MeV for the energy centroid. We find a width $\Gamma = 3.5$ MeV and an 80% depletion of the model-independent, energy-weighted sum rule (the calculations were carried out for $\Delta = 1$ MeV). The corresponding experimental values are[3] $\overline{E}_x = 13.46$ MeV, $\Gamma = 3.9$ MeV, and 89%, respectively. We see in Fig. 2 that the description of the experimental cross section is generally good. The cross section is overestimated somewhat at the maximum and underestimated somewhat at high energies. The reason is that in the actual calculations we were unable to include the large number of two-phonon states which are weakly coupled to the one-phonon states, because of the high density and also because of limitations in computer capability. To a large extent, the integral contribution of these neglected states can be taken into account by increasing the energy-averaging parameter $\Delta$. This figure also shows calculations of the distribution of the dipole strength in the random-phase approximation. We see from Figs. 1 and 2 that there is a substructure in the low-energy part of the cross section. The position of this substructure is very nearly the same as that of collective states in the random-phase approximation. The coupling to two-phonon states leads to a redistribution of the dipole strength. In the low-energy region, where the density of states is relatively low, the substructure is better defined. In the high-energy region, the cross sections are completely smooth. In nuclei far from the magic region there is a strong coupling between simple configurations and complex configurations, and the level density is high. Consequently, substructure is not observed.[7,16]

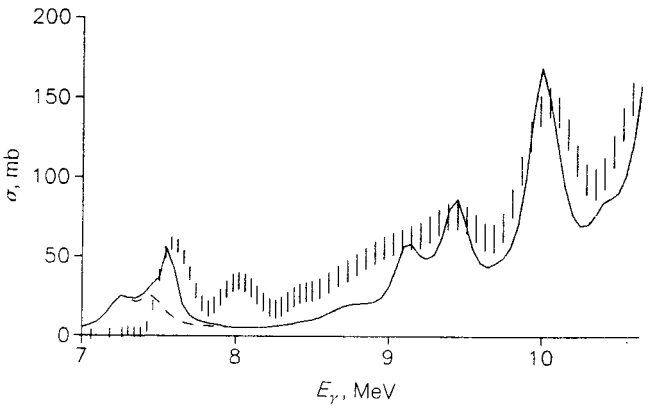


FIG. 3. Low-energy part of the $^{208}$Pb$(\gamma,n)$ cross section. Points—experimental; solid line—theoretical sum of the cross sections for $E1$ and $M1$ photoabsorption, with $\Delta = 0.2$ MeV.

As we mentioned earlier, the substructure is seen most clearly in the low-energy region of the tail of the giant dipole resonance (Fig. 3). To resolve the substructure question, we carried out some calculations with a smaller value of the energy-averaging parameter in this region. Figure 3 shows the results of our calculations of cross sections with $\Delta = 0.2$ MeV; this figure corresponds roughly to the experimental conditions. The theoretical results reproduce the basic substructural features at excitation energies of 7.6, 8.6, 9.1, 9.5, 10, and 11.3 MeV (Table I). The $M1$ isovector resonance which was studied by the quasiparticle–phonon model in Ref. 33 contributes substantially to the substructural feature at 7.6 MeV, along with $E1$ transitions (the dashed line). This result agrees well with experimental data obtained with polarized tagged photons.[34] The substructural feature at 8 MeV is not reproduced in our calculations, although Fig. 3 does reveal a double-humped structure in the $E1$ cross section at a lower energy. Our "old" calculations[7] also indicate two peaks in the interval 7–8 MeV. These differences appear to be a consequence of errors in the one-particle energies. However, we did not attempt to achieve an ideal description of the experimental data. We used the one-particle spectrum from our previous study. The contribution of $E2$ transitions to the photoneutron cross section is essentially indistinguishable against the $E1$ background.

## 6. CONCLUSION

It can be concluded from this study that intermediate structural features can be identified quite reliably in the low-energy part of the photoneutron cross section of $^{208}$Pb. Microscopic calculations reproduce the structural features in the experimental cross sections quite well. These calculations make it possible to identify these features as resulting from a nonuniform distribution of the dipole strength, which is itself a consequence of particular features of the one-particle spectrum and of the interaction between collective and noncollective degrees of freedom in this nucleus.

[1)]Institute of Mechanics and Physics, Saratov State University.

[1]K. Goeke and J. Speth, Ann. Rev. Nucl. Part. Sci. **32**, 65 (1982).
[2]A. Van der Woude, Prog. Part. Nucl. Phys. **18**, 217 (1987).
[3]B. L. Berman and S. C. Fultz, Rev. Mod. Phys. **47**, 713 (1975).
[4]S. N. Belyaev *et al.*, Izv. Akad. Nauk SSSR, Ser. Fiz. **48**, 1940 (1984).
[5]S. N. Belyaev *et al.*, Yad. Fiz. **42**, 1050 (1985) [Sov. J. Nucl. Phys. **42**, 662 (1985)].
[6]R. Van der Vyver *et al.*, Z. Phys. A **284**, 91 (1978).
[7]V. G. Soloviev *et al.*, Nucl. Phys. **A304**, 503 (1978).
[8]V. G. Soloviev *et al.*, Nucl. Phys. **A288**, 376 (1977).
[9]R. De Haro *et al.*, Nucl. Phys. **A388**, 265 (1982).
[10]G. Bertsch *et al.*, Rev. Mod. Phys. **55**, 287 (1983).
[11]V. N. Tkachev and S. P. Kamerdzhiev, Yad. Fiz. **42**, 832 (1985) [Sov. J. Nucl. Phys. **42**, 527 (1985)].
[12]V. V. Pal'chik *et al.*, Yad. Fiz. **34**, 903 (1981) [Sov. J. Nucl. Phys. **34**, 504 (1981)]; **35**, 1374 (1982); **35**, 801 (1982)].
[13]V. I. Bondarenko and M. G. Urin, Yad. Fiz. **46**, 1068 (1987) [Sov. J. Nucl. Phys. **46**, 617 (1987)].

[14]V. G. Solov'ev, Fiz. Elem. Chastits At. Yadra **9**, 860 (1978) [Sov. J. Part. Nucl. **9**, 343 (1978)].
[15]A. I. Vdovin and V. G. Solov'ev, Fiz. Elem. Chastits At. Yadra **14**, 237 (1983) [Sov. J. Part. Nucl. **14**, 99 (1983)].
[16]V. V. Voronov and V. G. Solov'ev, Fiz. Elem. Chastits At. Yadra **14**, 1380 (1983) [Sov. J. Part. Nucl. **14**, 583 (1983)].
[17]O. V. Bogdakevich and F. A. Nikolaev, *Working with a Bremsstrahlung Beam* [in Russian] (Atomizdat, Moscow, 1964).
[18]S. N. Belyaev *et al.*, Prib. Tekh. Eksp., No. 1, 18 (1980); No. 1, 21 (1981).
[19]S. N. Belyaev *et al.*, *Questions of Theoretical Nuclear Physics* [in Russian] (Saratov State University, Saratov, 1982).
[20]S. N. Belyaev *et al.*, *Abstracts, 32nd Conference on Nuclear Spectroscopy and Nuclear Structure* [in Russian] (Nauka, Leningrad, 1982), p. 370.
[21]V. F. Turchin *et al.*, Usp. Fiz. Nauk **102**, 345 (1970) [Sov. Phys. Usp. **13**, 681 (1971)]; Dokl. Akad. Nauk SSSR **212**, 561 (1973).
[22]P. Carlos *et al.*, Nucl. Phys. **A172**, 437 (1971).
[23]D. M. Blatt and V. F. Weisskopf, *Theoretical Nuclear Physics* (Wiley, New York, 1952) [Russ. transl., IL, Moscow, 1954].
[24]A. Veyssiere *et al.*, Nucl. Phys. **A159**, 91 (1970).
[25]P. Carlos *et al.*, *Electromagnetic Interactions of Nuclei at Low and Intermediate Energies* [Russian translation] (Nauka, Moscow, 1976).
[26]R. R. Harvey *et al.*, Phys. Rev. **136**, B126 (1964).
[27]B. S. Ishkhanov *et al.*, Yad. Fiz. **12**, 682 (1970) [Sov. J. Nucl. Phys. **12**, 370 (1970)].
[28]V. Yu. Ponomarev *et al.*, Preprint R-4-81-704, JINR, Dubna, 1981.
[29]V. V. Voronov and Dao Tien Khoa, Izv. Akad. Nauk SSSR, Ser. Fiz. **48**, 2008 (1984).
[30]V. A. Chepurnov, Yad. Fiz. **6**, 955 (1967) [Sov. J. Nucl. Phys. **6**, 696 (1968)].
[31]V. V. Voronov *et al.*, Yad. Fiz. **51**, 79 (1990) [Sov. J. Nucl. Phys. **51**, 49 (1990)].
[32]V. V. Voronov and V. Yu. Ponomarev, Nucl. Phys. **A520**, 619 (1990).
[33]Dao Tien Khoa *et al.*, Preprint E-4-86-198, JINR, Dubna, 1986.
[34]R. M. Laszewski *et al.*, Phys. Rev. Lett. **61**, 1710 (1988).

Translated by D. Parsons